E-Journal of Advanced Maintenance Vol.8-2 (2016) 32-42
Japan Society of Maintenology

Development of Resilience Evaluation Method for Nuclear Power Plant (Part 2: Development of Failure Probability Assessment Model for Static Components)

Masayuki KAMAYA[1,*] and Takao NAKAMURA[2]

[1] *Institute of Nuclear Safety System, Inc., 64 Sata, Mihama-cho, Fukui 919-1205, Japan*

[2] *Osaka University, 2-1 Yamadaoka, Suita, Osaka 565-0871, Japan*

ABSTRACT

Resilience index is proposed to be applied to evaluate the capability to recover safety performance of systems under severe accident of nuclear power plant. A failure probability assessment model was developed for the resilience evaluation of static components in nuclear power plants. This model took into consideration the effect of material degradation caused by low-cycle fatigue. NPP components consist of dynamic and static components, and this model focused on static components. Crack initiation due to fatigue damage was assumed and its depth was determined by the magnitude of fatigue damage. Then, crack growth was predicted for seismic loads consisting of a main quake and aftershocks. Finally, the failure probability was calculated for the seismic load. The fracture strength of the cracked component was calculated according to the fitness-for-service code, which took into account scatter in the flow stress. The developed model was successfully applied to a pipe of the residual heat removal system of a pressurized water reactor power plant. It was shown that the failure probability was hardly affected by the degree of fatigue damage, and that it was about 8.7×10^{-4} when the applied stress was equivalent to the maximum allowable stress for the component design. Although the crack depth had little influence on the fracture strength of the cracked pipe, an increase in the number of aftershocks could increase the probability of leakage.

KEYWORDS

failure probability, *low-cycle fatigue*, *seismic load*, *crack growth*, *aftershock*, *residual heat removal system*

ARTICLE INFORMATION

Article history:
Received 3 February 2016
Accepted 24 May 2016

1. Introduction

In the design of nuclear power plant (NPP) components, it is confirmed that the stress acting on the components does not exceed the material strength [1][2]. In order to secure further integrity of the components, it is important to consider the structural integrity for a load magnitude greater than that assumed in the design (hereafter, beyond design (BD) load). The NPP system has its own resilience for recovering from damage due to BD events. In order to assess the robustness of the system for the BD load, the failure probability of the components must be quantified.

Although the failure strength for the BD load can be estimated in the same way as for the component design, additional considerations are required for operating NPPs. Since various aging phenomena may reduce the failure strength of NPP component subjected to long-term operation, reduction in the failure probability due to the aging phenomena should be taken into account. In our previous study [3], it was pointed out that low-cycle fatigue is a degradation phenomenon that can affect the failure probability of static components. Low-cycle fatigue damage may initiate a crack and reduce the failure strength of components. It should be noted that changes in failure strength due to low-cycle fatigue need not to be considered when the plant operation conditions are within those considered in the design. This is because the degree of accumulated low-cycle fatigue damage is monitored during plant operation so that the accumulated damage is smaller than that predicted in the design. However, the influence of low-cycle fatigue damage must be taken into account for BD conditions.

In this study, an assessment model was developed for calculating the failure probability of static

*Corresponding author, E-mail: kamaya@inss.co.jp

ISSN-1883-9894/10

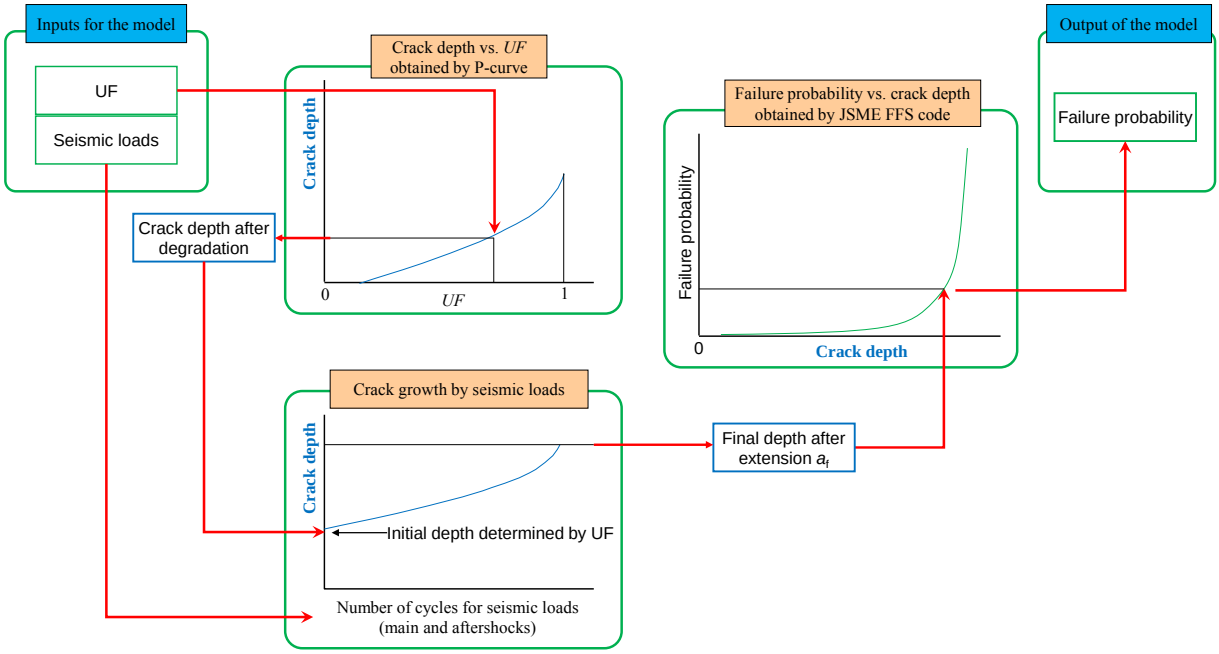

Fig. 1 Assessment procedure for calculating the failure probability of components subjected to beyond design loads.

components considering low-cycle fatigue damage during plant operation. This model is aimed at the application to resilience analyses [4] for DB conditions. The basic concept of this model has been shown in the previous study [4] and seismic loads were chosen as the BD conditions. Fatigue damage initiates a crack and the initiated crack may bring about component failure (fracture or leakage). The first step in assessing the failure probability was to calculate the depth of the crack caused by the low-cycle fatigue damage. The degree of fatigue damage is quantified using the usage factor (*UF*) in the plant design and maintenance. The component is considered to be safe when the *UF* is less than unity. However, a small crack may be initiated even when the *UF* is less than unity [5][6]. Therefore, in this model, a crack was assumed to exist regardless of the *UF* and the crack depth was determined using the postulated fatigue crack growth curve developed in our previous study [7]. Second, crack growth due to seismic loads was calculated. The equivalent stress intensity factor was used to predict the fatigue crack growth for large cyclic load caused by the BD loads. Third, the fracture strength of the components was calculated according to the fitness-for-service (FFS) assessment procedure prescribed in the FFS code for nuclear power plant components issued by the Japan Society of Mechanical Engineers (JSME) [8]. By considering the scatter in material strength, the failure probability of the components was obtained. Finally, the model was applied to calculate the failure probability of a pipe of the residual heat removal system, which is a key system for recovering from core damage accidents in various scenarios [3]. The influence of the material strength distribution and the effect of the cyclic load caused by aftershocks was also discussed.

2. Failure Probability Assessment Model

2.1. Overview

The failure probability of the components was calculated according to the procedure schematically shown in Fig. 1. Inputs to the model were external hazard, represented by the seismic loads, and degree of fatigue damage accumulated in the component, which was represented by the *UF*. A crack was postulated in the assessment. The crack depth was determined from the *UF* using the postulated crack growth curve (hereafter referred to as P-curve), which is described in detail in the next section. The crack was extended by seismic loads, which consisted of a main quake and aftershocks. The fracture strength of the cracked component was calculated according to the JSME FFS code. Then, the failure

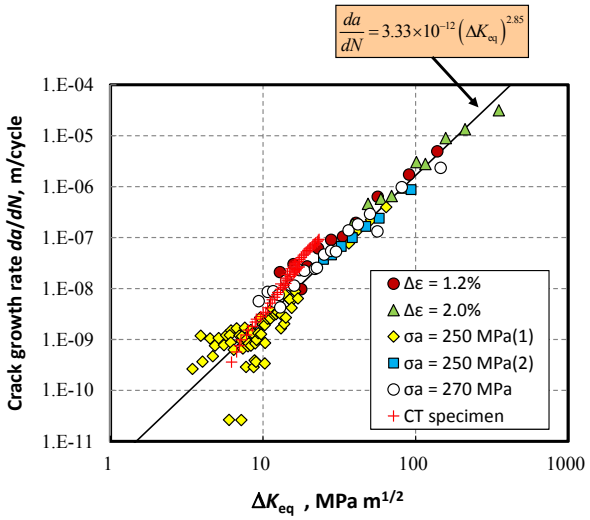

Fig. 2 Low- and high-cycle fatigue crack growth rates obtained using Type 316 stainless steel.

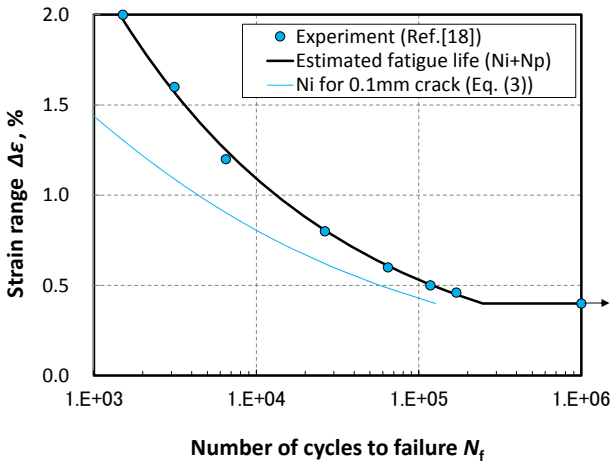

Fig.3 Fatigue life estimated by crack growth analysis together with the fatigue life obtained by low-cycle fatigue tests.

probability was derived by considering the scatter in material strength in the fracture strength calculation. An important characteristic of the model is that the failure probability can be calculated using an Excel sheet without any macros. Therefore, the model can easily be combined with the resilience evaluation model [9]. The details of each assessment are explained in the following subsections.

2.2. Postulated crack growth curve (P-curve)

In order to determine the crack depth for a given *UF*, the P-curve has been developed by the present authors [10][11]. The *UF* is determined using the fatigue life obtained by fatigue tests. It has been shown that small cracks less than tens of micrometers in length are initiated at the early stage of fatigue tests. Then, for a Type 316 stainless steel at room temperature, the growth rate for small cracks was obtained as [12]:

$$\frac{da}{dN} = 3.33\times10^{-12}\left(\Delta K_{eq}\right)^{2.85}. \quad (1)$$

The growth rate da/dN is given in m/cycle and ΔK_{eq} in MPa $m^{0.5}$. ΔK_{eq} is the equivalent stress intensity factor defined by:

$$\Delta K_{eq} = f\,\Delta\varepsilon E\sqrt{\pi a} \quad (2)$$

where $\Delta\varepsilon$ is the applied strain range, a is the crack depth and f is the geometrical constant [12]. E is Young's modulus and E = 195 GPa was applied for room temperature. The growth rates obtained using compact tension (CT) specimens under small scale yielding conditions are also shown in Fig. 2. The measured crack growth rates correlated well with ΔK_{eq} regardless of the loading amplitude and yielding conditions [13]-[15]. The growth rate predicted by Eq. (1) is applicable to both high- and low-cycle regimes regardless of the stress and strain amplitude. The fatigue life of stainless steel correlated well with the strain range rather than the stress range [16]-[19]. The equivalent stress intensity factor together with Eq. (1) enables the crack growth for a given strain range to be predicted without considering the stress amplitude.

Crack growth was predicted for a given strain range assuming an initial crack depth of 0.1 mm and an incubation period N_i determined by [10]:

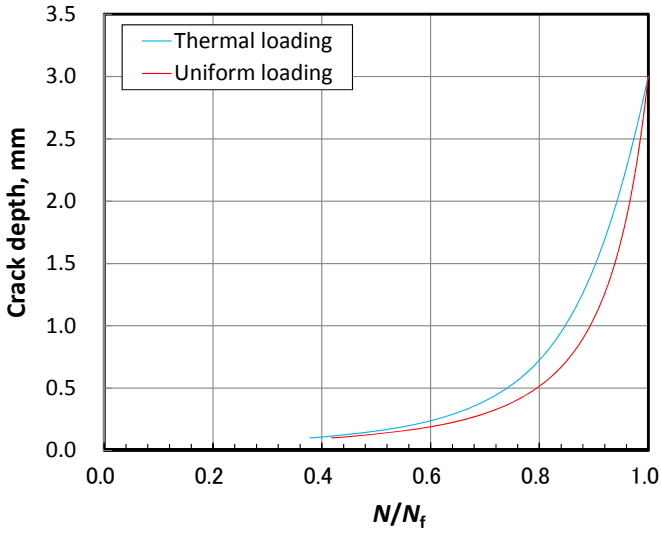

Fig.4 Change in crack depth with normalized number of cycles obtained for uniform and thermal loading conditions (P-curve).

$$N_i = 3948\left(\Delta\varepsilon[\%]\right)^{-3.95}. \quad (3)$$

The fatigue life corresponds to the sum of N_i and the number of cycles for an initiated 0.1 mm deep crack growing to 3 mm deep. Figure 3 shows the estimated fatigue life together with the fatigue life obtained by low-cycle fatigue tests [20]. The fatigue life estimated using Eqs. (1) and (3) agree well with that obtained experimentally.

Figure 4 shows the change in crack depth with the number of cycles normalized by the estimated fatigue life N/N_f obtained for a strain range of $\Delta\varepsilon$ = 0.8%. N/N_f defined for the fatigue tests corresponds to the *UF* obtained for the actual component. Therefore, it is possible to determine the crack depth for a given *UF* by replacing N/N_f with *UF* in Fig. 4. Since the maximum crack depth for the fatigue test is approximately 3 mm [12], the crack depth does not exceed 3 mm when $UF < 1$. The curve shown in Fig. 4 corresponds to the P-curve.

Most of the fatigue damage considered in the component design of nuclear power plants is brought about by fluid temperature fluctuations caused by changes in operating mode. The cyclic stress and strain due to the fluid temperature fluctuation on a component surface forms a gradient in the depth direction [21]. The P-curve considering the stress gradient in the crack growth prediction is also shown in Fig. 4 [10]. The thermal stress was calculated assuming ramp change in fluid temperature on the surface. The incubation period of a 0.1 mm deep crack was determined by Eq. (3) and growth prediction was made using Eq. (1). The crack depth obtained for the thermal load is larger than that obtained for the uniform stress.

2.3. Crack growth by seismic loads

Cyclic loads caused by the seismic loads propagate the crack initiated by fatigue damage. In the model, crack growth due to seismic loads is estimated using the equivalent stress intensity factor. As mentioned, the equivalent stress intensity factor is applicable to the crack growth prediction for a large cyclic load exceeding the small scale yielding conditions [15]. The cyclic loadings are caused not only by the main quake but also by aftershocks. The strain range for calculating the equivalent stress intensity factor is derived from the stress range using the plastic strain correction factor K_e used for the component design [2]. Crack depth after the growth analysis is denoted by a_f and is subjected to the failure assessment. If a_f exceeds 75% of the component thickness t, the crack is judged to be a leakage failure.

2.4. Failure probability

The failure load of the cracked component is calculated according to the JSME FFS code. Stainless

steel is commonly used for nuclear power plants and the failure mode of the stainless steel assumed in the JSME FFS code is plastic collapse. The maximum bending load (limit load) of the cracked pipe for plastic collapse failure is calculated by [8]:

$$P_b' = \frac{2S_f}{\pi}\left(2\sin\beta - \frac{a_f}{t}\sin\frac{c}{R_i}\right) \tag{4}$$

$$\beta = \frac{1}{2}\left(\pi - \frac{a_f}{t}\frac{c}{R_i} - \pi\frac{P_m}{S_f}\right) \tag{5}$$

where c and R_i are the half crack length and the pipe inner radius, respectively. P_m is the axial load and S_f is the flow stress, for which the average yield and ultimate strength are applied in the JSME FFS code [8].

The applied load is assumed to be the same as the maximum peak load caused by the seismic load. If the applied load is larger than the limit load P_b', the pipe is judged to have failed. In the model, the variations in flow stress are considered, and then the failure probability is calculated.

4. Assessment for Residual Heat Removal System

The failure probability assessment model was applied to the residual heat removal (RHR) system. The RHR system plays an important role in the recovery from reactor core damage accidents [3]. The detailed assessment conditions are as follows.

4.1. Geometrical, operational and material conditions

The geometrical and operational conditions applied to the assessment are summarized in Table 1. This data corresponds to a piping system of the RHR system. The material constants used in the assessment were obtained from the JSME codes for material [22] and are shown in Table 2. As mentioned, the inputs required for deriving the failure probability are the *UF* and seismic loads. The maximum peak stress of the seismic load is represented by:

$$P_m + P_b = \alpha S_y \tag{6}$$

where S_y is the yield strength value defined in the design code [22] and α is the constant. In the design of Class 1 components of NPPs, the sum of the membrane stress P_m and bending stress P_b caused by seismic load is confirmed to be less than $2S_y$ [23]. Namely, $\alpha = 2$ means the maximum stress condition considered in the component design and $\alpha > 2$ corresponds to BD conditions.

Table 1 Geometrical and operational conditions for RHR system

Operation temperature	200°C
Internal pressure: P_i	5 MPa
Pipe material	SUS304TB
Outer diameter: D_o	267.4 mm (10B)
Thickness: t	15.1 mm (Sch 80)

Table 2 Material strength obtained from JSME material code [22] (200°C)

Young's modulus: E	183 GPa
Design stress intensity value: S_m	129 MPa
Yield strength value: S_y	144 MPa
Tensile strength value: S_u	402 MPa
Flow stress: $S_f = (S_y + S_u)/2$	273 MPa

4.2. Crack growth analysis

The initial depth a of the postulated crack was determined from the given UF using the P-curve shown in Fig. 4. The surface length of the crack $2c$ was assumed to be $2c = a$. The initial crack was extended by the seismic loads. To calculate the equivalent stress intensity factor, the strain range corresponding to the applied load given by Eq. (6) was determined using the plastic strain correction factor K_e. In the JSME design code [2], the value of K_e is obtained by:

$$K_e = 1 + 0.7\left(\frac{S_n}{2S_y} - 1\right) \text{ when } \frac{S_n}{S_y} < 1 \tag{7}$$

$$K_e = 1 + 2.1\left(1 - \frac{2S_y}{S_n}\right) \text{ when } \frac{S_n}{S_y} \geq 1 \tag{8}$$

where S_n is the range of the membrane and bending stress fluctuations and it was assumed to be $2(S_m + S_b)$. Thus, the strain range $\Delta\varepsilon$ is calculated by:

$$\Delta\varepsilon = \frac{S_n}{E} \times K_e \,. \tag{9}$$

The geometrical constant f for the equivalent stress intensity factor was set to 0.82, which corresponds to the geometrical constant for a circumferential inner surface crack of $a/t = 0.2$ [7]. Then, the crack growth rate is calculated by:

$$\frac{da}{dN} = 2.93 \times 10^{-12} \left(\Delta K_{eq}\right)^{3.3} . \tag{10}$$

This equation corresponds to the fatigue crack growth rate in an air environment at 200°C given in the JSME FFS code appendix E-2-10 [8]. The stress ratio R was assumed to be $R = -1$. The number of cycles caused by the main quake was assumed to be 60 [24]. Also, the same number of cycles and magnitude of cyclic loads were applied for a single aftershock. Namely, two aftershocks caused 120

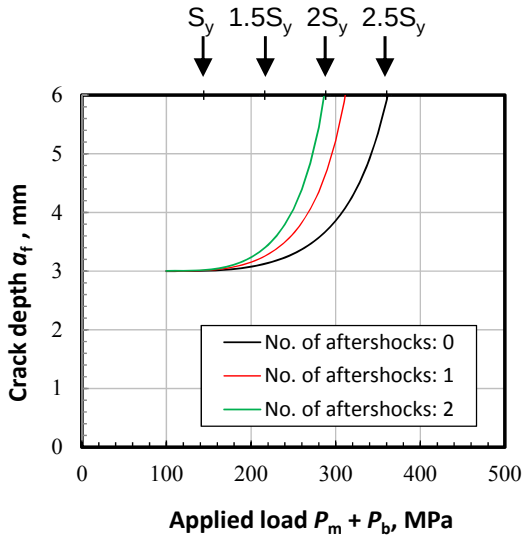

Fig. 5 Change in crack depth with applied load (UF = 1).

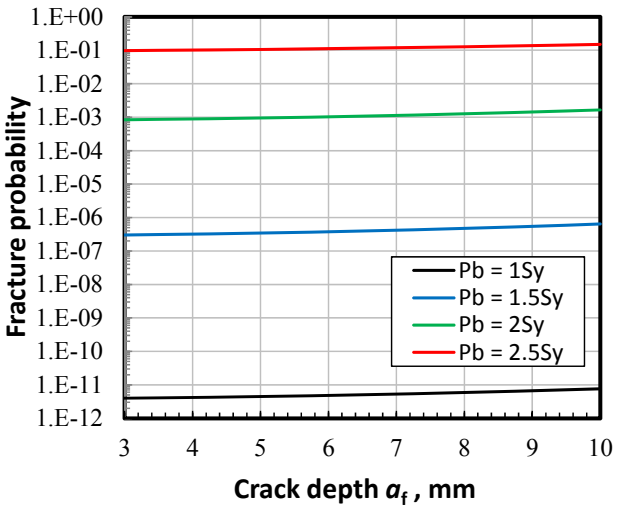

Fig. 6 Fracture probability calculated by the JSME FFS code.

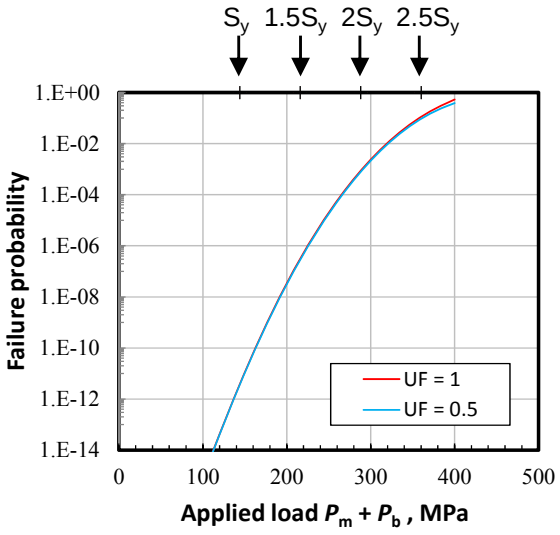

Fig. 7 Change in failure probability with applied load obtained for *UF* = 1.0 and 0.5 (No. of aftershocks = 0).

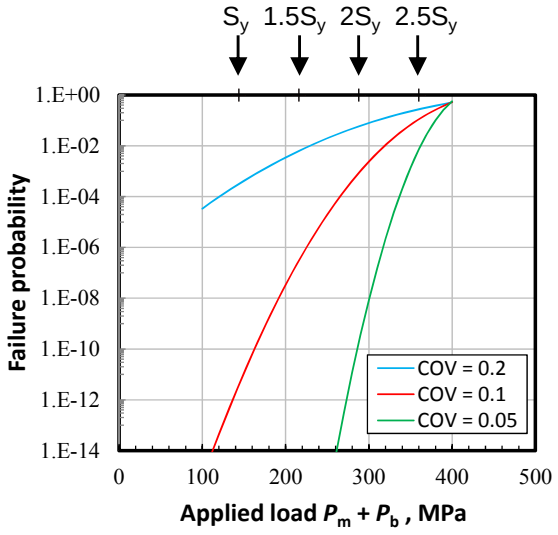

Fig. 8 Change in failure probability with applied load obtained for various *COV*s (*UF* = 1, No. of aftershocks = 0).

cycles of crack growth in addition to 60 cycles by the main quake. The crack was extended in the depth direction while the surface length was kept at $2c = a$.

Figure 5 shows the change in crack depth after growth by the seismic loads. The *UF* was assumed to be $UF = 1$. Namely, the crack depth before the growth analysis was 3 mm. The crack depth a_f became deeper as the applied load was increased. The depth was $a_f = 3.68$ mm when the applied load was $2S_y$ without considering aftershocks. The depth became $a_f = 6.12$ mm when two aftershocks were considered. If the crack depth a_f exceeded 75% of the pipe wall thickness, which was $t = 15.1$ mm, the crack was judged to penetrate the wall thickness. This is an engineering treatment in the structural integrity assessment of cracked pipes [8].

4.3. Fracture analyses

If the applied bending stress P_b exceeds the limit load P_b', the pipe is judged to have failed due to plastic collapse. The material parameter determining the limit load is the flow stress S_f. In the assessment, the variation in flow stress was considered. The magnitude of the variation was represented by *COV* (coefficient of variation: standard deviation/mean value). The values of S_y and S_u were determined by multiplying the test results by 0.885 for a conservative design [2]. If the variation between S_y, S_u and the test results corresponds to 3σ of the normal distribution, the *COV* for S_y and S_u is $(1 - 0.885)/3 = 0.038$. The FFS code of API (American Petroleum Institute) [25] states that the minimum yield strength used for the assessment should be 69 MPa lower than the yield strength obtained by material tests. If 69 MPa corresponds to 3σ, the *COV* for flow stress is $69/(3 \times 273) = 0.084$. Then, in this model, the *COV* and mean value of the flow stress were assumed to be 0.1 and 273/0.885 = 308.5, respectively.

Figure 6 shows the change in fracture probability with crack depth. The minimum flow stress required for a given crack depth and applied bending stress can be derived using Eqs. (4) and (5). The membrane stress was assumed to be caused by internal pressure, which was half the hoop stress $0.5P_i \times R_m/t$. The fracture probability was calculated as the cumulative probability for S_f. As shown in Fig. 6, the fracture probability greatly depended on the applied load and hardly depended on the crack depth. The limit load largely depends on the net section area, which is the uncracked area on the cracked cross section. The change in net section area due to crack growth was not significant and had little influence on the change in limit load. The failure probability was about 0.1% regardless of the crack depth when the bending stress of $P_b = 2S_y$ was applied.

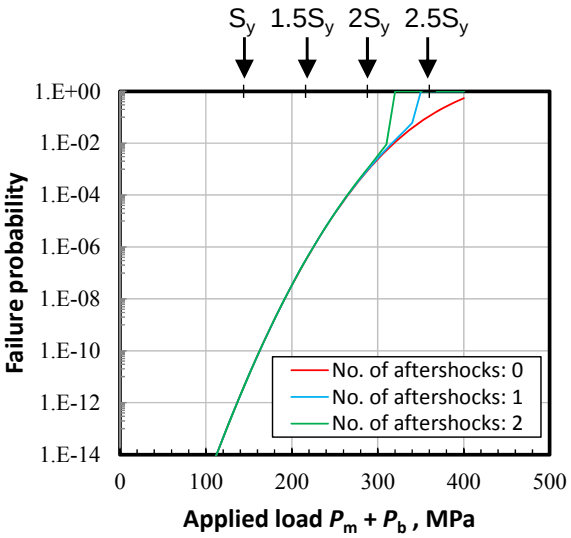

Fig. 9 Change in failure probability with applied load obtained for various number of aftershocks (*UF* = 1).

4.4. Analysis results

The fracture probability was obtained for the crack depth as shown in Fig. 6. On the other hand, the crack depth a_f was obtained by the crack growth analysis for the seismic loads. Then, by using a_f for the fracture probability calculation shown in Fig. 6, the failure probability (probability of leakage or fracture) was obtained as shown in Fig. 7, for which growth by aftershocks was not considered. The failure probability greatly depended on the magnitude of applied load and was about 8.7×10^{-4} when $P_m + P_b = 2S_y$. The failure probabilities obtained for $UF = 1.0$ and 0.5 were almost identical. The initial depth used for $UF = 0.5$ was 0.158 mm, which was obtained for the uniform loading conditions shown in Fig. 4, whereas it was 3 mm for $UF = 1$. Although the initial depth of $UF = 0.5$ was much less than that of $UF = 1$, the failure probability was almost the same. Since the fracture probability hardly depended on the crack depth as shown in Fig. 6, the failure probability had little dependency on the *UF*. In the analyses shown in Fig. 7, the crack depth a_f did not reach $0.75t$.

Figure 8 shows the change in failure probability for different variations in flow stress obtained for $UF = 1$. A larger scatter in flow stress resulted in a higher failure probability. This implies that the variation in material strength should be suppressed in order to reduce the failure probability.

The change in failure probability with a different number of aftershocks is shown in Fig. 9 for $UF = 1$. The number of aftershocks had little influence on the failure probability when $P_m + P_b$ was less than $2S_y$. The failure probability for larger applied stress increased abruptly when the number of aftershocks was one or two. This was due to crack penetration of the wall thickness. The crack depth after the growth analysis became larger than $0.75t$ when the number of cycles was large.

5. Discussion

As mentioned, the failure probability calculation by the developed model can be performed on an Excel sheet without any macros. Figure 10 shows the Excel sheet for calculating the failure probability. The red characters indicate values to be given by the user. In other words, these parameters can be changed arbitrarily. The failure probability is derived for each applied load $P_m + P_b$. Crack growth by seismic load can be calculated using a single equation when the geometrical constant *f* for calculating the equivalent stress intensity factor is a fixed value regardless of the crack depth [5]. Then, for simplicity, the fixed value of $f = 0.82$ was used in this study.

It should be noted that stress corrosion cracking (SCC) is also a major degradation phenomenon that occurs in NPP components. Therefore, cracking due to SCC may reduce the fracture strength of the

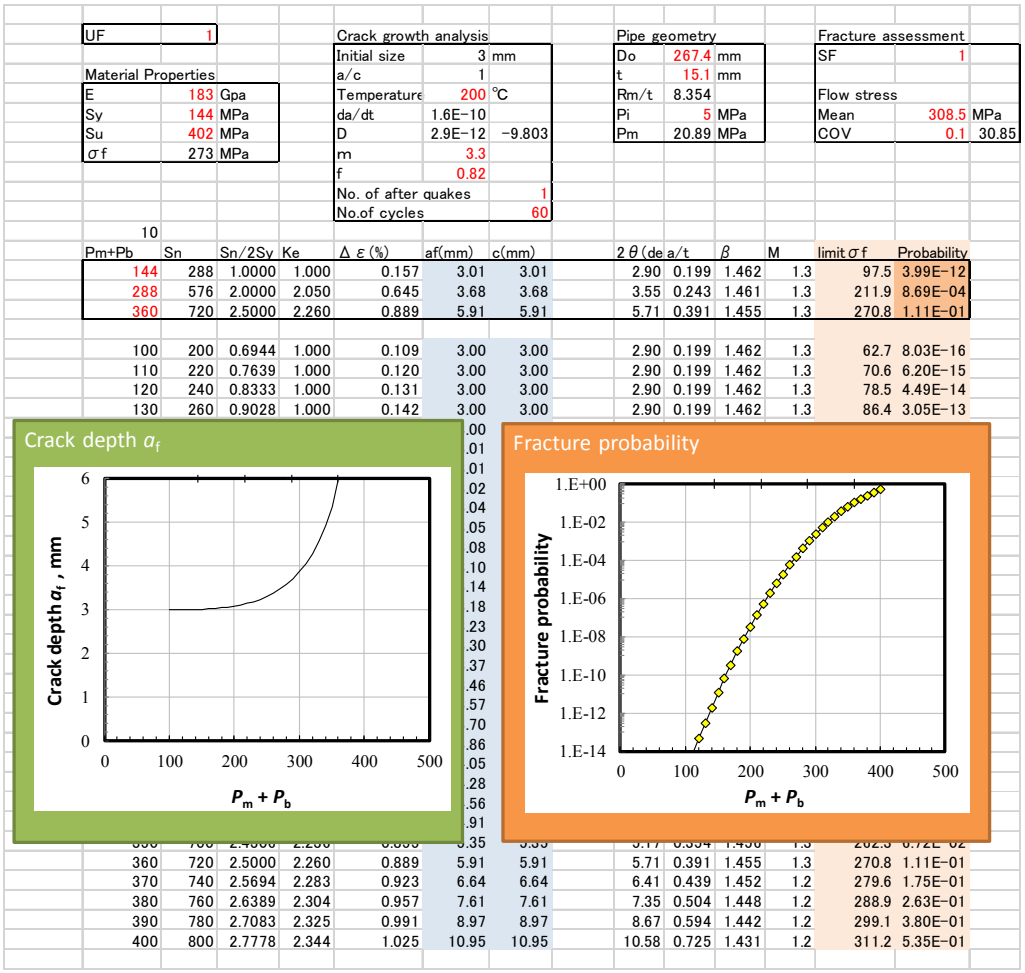

Fig. 10 Excel file for calculating failure probability.

component. The magnitude of damage induced by SCC can also be represented by the crack depth as in the case for fatigue damage, so it is relatively easy to take the effect of SCC into account in the failure probability assessment model. Since SCC is not generally initiated in the stainless steel pipes of pressurized water reactor NPPs, the effect of SCC was not considered in this study. It should be noted that efforts to prevent SCC are taken in the component design, whereas accumulation of fatigue damage is assumed. Therefore, if SCC is successfully prevented, it need not be considered in the failure probability assessment model.

6. Conclusion

In order to calculate the failure probability for the resilience evaluation of NPP static components, failure probability assessment model was developed. This model could consider material degradation due to low-cycle fatigue damage accumulated during plant operation. The magnitude of the fatigue damage was quantified by the crack depth using the P-curve together with the *UF*. After the analysis of growth due to the seismic loads, the crack was subjected to fracture strength assessment according to the JSME FFS code. Then, the failure probability of the component was quantified. This model was successfully applied to the RHR system, which is the key system in various scenarios for recovering from core damage accidents. The failure probability was about 8.7×10^{-4} when $P_m + P_b = 2S_y$, which corresponded to the maximum stress considered in the design. A larger scatter in the flow stress resulted in a higher failure probability. It was revealed that the failure probability was hardly affected by the magnitude of *UF*. Although the initial crack depth and crack growth due to seismic loads had little influence on the failure probability, the increase in the number of aftershocks increased the failure probability because the crack penetrated the wall thickness during the aftershocks.

Acknowledgement

This work has been performed as a part of the Japan Ageing Management Program on System Safety (JAMPSS) sponsored by the Nuclear Regulation Authority (NRA).

References

[1] ASME, "Rules for Construction of Nuclear Facility Components – ASME Boiler and Pressure Vessel Code Section III", ASME, New York (2013).
[2] Japan Society of Mechanical Engineers, "Codes for Nuclear Power Generation Facilities: Rules on Design and Construction for Nuclear Power Plants", JSME S NC1-2012 (2012).
[3] T. Nakamura, M. Kamaya, "Development of resilience evaluation method for nuclear power plant (part 2: study on reliability analytical method for degradation of static components)", Maintenology, Vol. 15, pp.71-76 (2016).
[4] K. Demachi, M. Suzuki, T. Itoi, K. Murakami, N. Kasahara, H. Miyano, T. Nakamura, S. Arai, M. Kamaya, A. Yamaguchi, M. Matsumoto, "Development of resilience evaluation method for nuclear power plant (part 1: proposal of resilience index for assessment of safety of nuclear power plant under severe accident)", Maintenology, Vol. 15, pp.65-70 (2016).
[5] M. Kamaya, M. Kawakubo, "Strain-based modeling of fatigue crack growth – An experimental approach for stainless steel", International Journal of Fatigue, Vol. 44 pp.131-140 (2012).
[6] S. Abe, T. Nakamura, M. Kamaya, "Statistical model of micro crack growth for the evaluation of accumulated fatigue in NPPs", E-Journal of Advanced Maintenance, Vol.7-1 pp.129-137 (2015).
[7] M. Kamaya, T. Nakamura, "A flaw tolerance concept for plant maintenance using virtual fatigue crack growth curve", Proceedings of the ASME 2013 Pressure Vessels and Piping Conference, Paris, France, July, paper no. 97851 (2013).
[8] Japan Society of Mechanical Engineers, "Codes for Nuclear Power Generation Facilities: Rules of Fitness-for-Service for Nuclear Power Plants", JSME S NA1-2012 (2012).
[9] M. Suzuki, K. Demachi, K. Murakami, T. Itoi, N. Kasahara, H. Miyano, T. Nakamura, S. Arai, M. Kamaya, A. Yamaguchi, M. Matsumoto, "Development of resilience evaluation method for nuclear power plant (part 3: study on evaluation method and applicability of resilience index)", Maintenology, in press.
[10] M. Kamaya, T. Nakamura, "Fatigue damage management based on postulated crack growth curve", E-Journal of Advanced Maintenance, Vol.7-1 pp.43-49 (2015).
[11] M. Kamaya, "Damage assessment of low-cycle fatigue by crack growth prediction (fatigue life under cyclic thermal stress)", Transactions of the Japan Society of Mechanical Engineers A, Vol. 79 pp.1530-1544 (2013).
[12] M. Kamaya, M. Kawakubo, "Damage assessment of low-cycle fatigue by crack growth prediction (development of growth prediction model and its application)", Transactions of the Japan Society of Mechanical Engineers Ser. A, Vol. 78 pp.1518-1533 (2012).
[13] J. R. Haigh, R. P. Skelton, "A strain intensity approach to high temperature fatigue crack growth and failure", Materials Science and Engineering, Vol. 36, pp.133-137 (1978).
[14] H. Kitagawa, S. Takahashi, C.M. Suh, S. Miyashita, "Quantitative analysis of fatigue process – microcracks and slip lines under cyclic strains", ASTM STP 675, pp.420-449 (1979).
[15] M. Kamaya, "Low-cycle fatigue crack growth prediction by strain intensity factor", International Journal of Fatigue, Vol. 72 pp.80-89 (2015).
[16] C. E. Jaske, W. J. O'Donnell, "Fatigue design criteria for pressure vessel alloys", ASME Journal of Pressure Vessel Technology, Vol. 99, pp.584-592 (1977).
[17] J. Colin, A. Fatemi, "Variable amplitude cyclic deformation and fatigue behavior of stainless steel 304L including step, periodic, and random loading", Fatigue & Fracture of Engineering Materials & Structures, Vol. 33, pp.205-220 (2010).
[18] M. Kamaya, M. Kawakubo, "Mean stress effect on fatigue strength of stainless steel", International Journal of Fatigue, Vol. 74 pp.20-29 (2015).
[19] M. Kamaya, M. Kawakubo, "Loading sequence effect on fatigue life of Type 316 stainless steel", International Journal of Fatigue, Vol. 81 pp.10-20 (2015).
[20] M. Kawakubo, M. Kamaya, "Fatigue life prediction of stainless steel under variable loading (damage factors determining fatigue life and damage evaluation for two-step test)", Journal of the Society of Materials Science, Japan, Vol. 60, pp.871-878 (2011).
[21] M. Kamaya, "Assessment of thermal fatigue damage caused by local fluid temperature fluctuation (Part I: Characteristics of constraint and stress caused by thermal striation and stratification)", Nuclear Engineering and Design, Vol. 268, pp.121-138 (2014).
[22] Japan Society of Mechanical Engineers, "Codes for Nuclear Power Generation Facilities: Rules on Materials

for Nuclear Facilities", JSME S NJ1-2012 (2012).
[23] Electric Association Nuclear Standards Board, "Seismic Design Technology Guidelines for Nuclear Power Station", JEAC 4601-2008 (2008), Japan Electric Association.
[24] Japan Nuclear Energy Safety, "Report of integrity of nuclear power plant components for seismic load: ultimate strength of piping system (in Japanese)", 04-KiKouHou-0002, p.4-8 (2004).
[25] American Petroleum Institute, "Fitness-for-Service, Second Edition API 579-1/ASME FFS-1", American Petroleum Institute (2007).